

A.N. Dyusembaeva<sup>1,2</sup>, N.K. Tanasheva<sup>1,2</sup>, A.Zh. Tleubergenova<sup>1,2</sup>, A.R. Bakhtybekova<sup>1,2\*</sup>,  
Zh.B. Kutumova<sup>1</sup>, A.R. Tussuphanova<sup>1,2</sup>, N.T. Abdirova<sup>1</sup>

<sup>1</sup>Karaganda Buketov University, Karaganda, Kazakhstan;

<sup>2</sup>Scientific Center "Alternative Energy", Karaganda, Kazakhstan

\*(Corresponding author's e-mail: asem.alibekova@inbox.ru)

## Optimal choice of the geometric shape rotor blade wind turbine using the numerical method

To increase the energy efficiency of wind turbines, it is necessary to optimize and improve the shape and size of power elements. In this work, in order to improve the output energy indicators, as well as increase the lifting force, a combined blade in the form of a rotating cylinder and a fixed blade was created and numerically studied. The novelty of the work lies in obtaining the results of the influence of a fixed angle of inclination of the blade on the overall aerodynamic characteristics of the entire combined blade at wind speeds from 3 to 12 m/s. Based on three-dimensional modeling, 4 variants of the combined blade with different angles of location are designed. Three-dimensional patterns of the distribution of velocity vectors and pressure fields are obtained. Linear graphs of the dependence of aerodynamic coefficients on the Reynolds number are shown. It was found that at an angle of 0 degrees, the combined blade has a maximum lift coefficient of 10 and a minimum drag coefficient of 4.5 at Reynolds  $1 \cdot 10^4$ . The numerical results obtained will be useful in the development of wind power plants with combined blades operating on the basis of Magnus.

*Keywords:* wind turbine, combined blade, cylinder, Magnus effect, geometric shape, aerodynamic force, three-dimensional modeling, Reynolds number.

### Introduction

When designing and creating a wind turbine, the main goal is to achieve maximum output power under specified atmospheric weather conditions. From a physical point of view, this is achieved by creating blades with optimal parameters and shapes. Changing the shape and linear dimensions of the blades affects the aerodynamic coefficients of a blade wind turbine. In the making of the blade, about 15–20% of the total cost of production of a wind turbine is spent. Nevertheless, the profit received from improving the structural model of the blade is tangible [1-2].

The selection and finding of a suitable blade shape and its material is a difficult task because the mathematical description of aerodynamic behavior is a complex process and requires several actions.

Currently, there are 3 types of wind turbine design (Fig. 1).

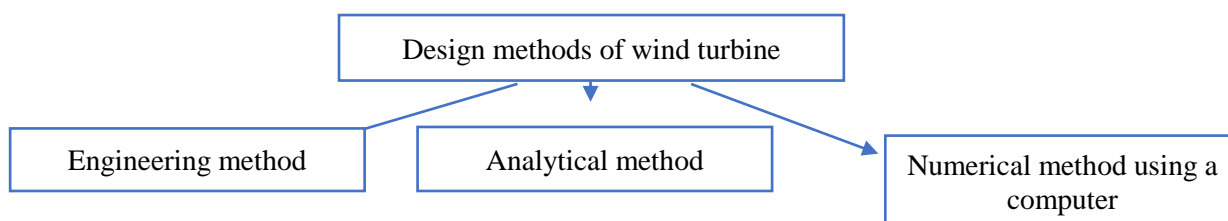


Figure 1. Design methods of wind turbine

Figure 1 shows that the first and third methods are often used in engineering practice when creating elements and wind turbines themselves. The analytical method can determine the characteristics of wind turbines, such as torque, shaft power, etc. The engineering method allows you to create a wind turbine with the best electrical characteristics. A numerical method can be used to obtain a picture of the airflow around wind turbines.

One of the most popular wind turbines in the world is the blade wind turbine. Nevertheless, in addition to the undeniable benefits, the wind generator has a major disadvantage in the form of a direction to the

wind. Designers and producers purposely hide this fact from consumers and only inform them about the benefits of the setup. But in practice, it turns out this way: the power of the wind turbine is defined on the basis that the wind direction always corresponds to the axis of rotation of the wind turbine, that is, the wind blows directly on the calculated surface of the blade. As a result, the calculated power of the wind turbine is received but in real life, the wind direction is not known to be constant [3].

Another type of wind turbine is installed with cylindrical blades, working based on the Magnus effect. Compared with vane wind turbines, these installations have the advantage of generating energy at low wind speeds ranging from 2-3 m/s, and there is no need for wind orientation. Thanks to the cylindrical blades, the wind potential of the air is captured, both from the windward side and the windward side, so there is no need for orientation in the wind direction [4].

The work's authors [5] modified the blade, which is a combination of blades in which an ordinary model in the shape of a circle is combined with a concave elliptical model. It was found that thanks to the combined blade, the power factor of the wind turbine ( $C_{max}$ ) increases to 11%, thereby improving the characteristics of the wind turbine.

It was determined in the work that after a certain length of the separation plate, a secondary vortex appears on the tail edge. It is determined that the rotation of the vortex is opposite to the main vortex and affects the formation of the primary vortex, as well as the formation of the shear layer [6]. However, these studies were conducted at low Reynolds numbers equal to 485.

The authors also found [7] that the longer the plate, a large value of the initial jump velocity is observed, the reason for this is a jump in the amplitude of vibration and fluctuations in lift. With the introduction of an upstream plate, boundary layers are formed along the plate before attaching to the surface of the cylinder.

In the work, the authors [8] investigated a cylinder equipped with three different separation plates and capable of oscillating across the incoming flow, with a range of Reynolds numbers from 1,500 to 16,000. The conducted studies confirm that the transverse jump mechanism is responsible for bringing cylinders with separation plates into high-amplitude vibrations.

The work [9] is devoted to the experimental study of the aerodynamic characteristics of round cylinders with small end plates and elongation in the critical range of Reynolds numbers. However, it is necessary to perform numerical control of the two-dimensional flow in the subcritical range.

Also, many works are devoted to the numerical study of cylinders of various shapes, such as square, rectangular and triangular [10–12]. In [13], the proposed approach allows us to quantitatively study the unsteady behavior of lifting force on vertical bodies with a complex shape.

Nevertheless, many works are devoted to the study of the flow around a cylinder with a plate, with the influence of the length and width of the plate [14–16]. But the works devoted to the study of the angle of the plate relative to the circular rotating cylinder at high Reynolds numbers are not enough.

Based on this, using design methods, the creation of a combined blade containing a cylinder and a traditional fixed blade, thereby combining two lifting forces, a fixed and cylindrical blade, and reducing the dependence of the cylinder rotation speed on wind speed, with subsequent investigation of the influence of the plate angular arrangement is an urgent issue [17–20].

There are known data on the effect of the relative length of the cylinder on the values of lift and drag. It is established that with the transverse flow of the cylinders, the influence of cylinder elongation on the coefficient of drag and lift is sufficiently exerted [17]. In this paper by the authors [18-19], if  $L/D=40$ , the value of the aerodynamic coefficient differs by 18% from the data of the infinite cylinder. Based on this, it can be concluded that to design optimal blade sizes, it is necessary to select optimal values of the length and diameter of the cylinder, and the angle of the fixed blade, based on previous work.

This article presents the results of a numerical study, focusing on the representation of aerodynamic coefficients depending on the Reynolds number and wind speed for 4 variants of the fixed blade relative to the cylinder.

The aim of the work is to conduct a numerical study of a combined blade containing a rotating cylinder and a fixed blade.

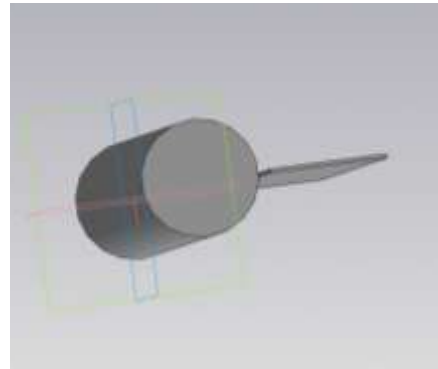
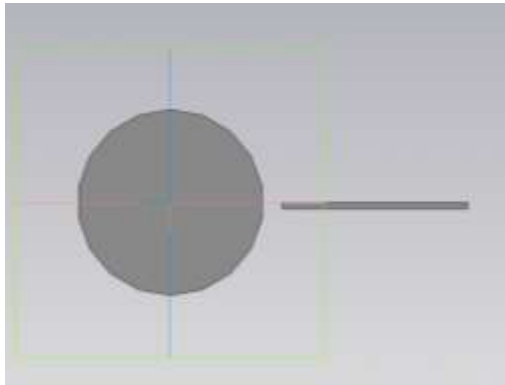
In accordance with the purpose of the study, the following tasks are formulated:

- development and creation of 4 versions of blades with tilt angles of 0, 30, 45 and 60 degrees;
- creation of computational domains with the setting of boundary conditions;
- obtaining the results of the pressure distribution fields and velocity vectors around the studied layout;
- obtaining dependencies of aerodynamic coefficients on the Reynolds number.

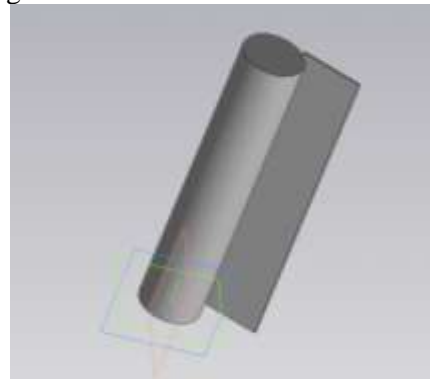
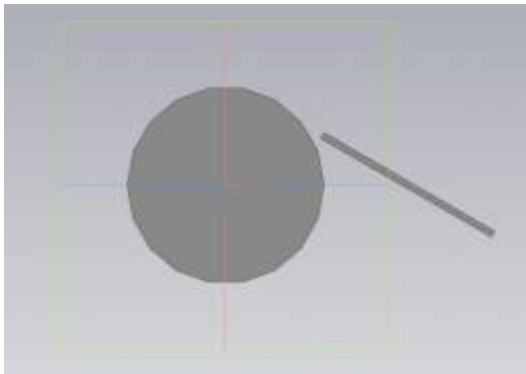
### Geometry features

Based on the existing works of well-known authors and engineers, 4 numerical models of blades with different angles of fixed blade arrangements were created using numerical modeling (Fig. 2). Focusing on the highly effective results of the well-known works of such several authors as N.K.Tanasheva and Dyusembaeva [19, 21-22], an optimal cylindrical blade with a diameter of 50 mm and a length of 300 mm was created. The width of the fixed blade was 33 mm, and the length was 300 mm.

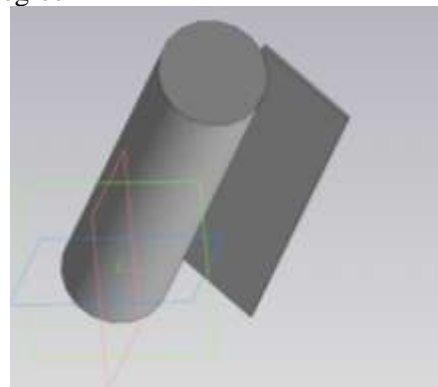
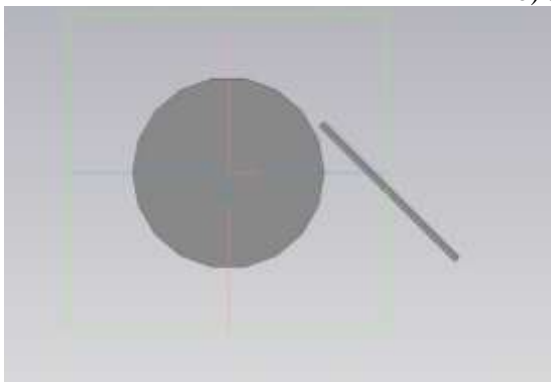
A numerical simulation was carried out to find the optimal angle of the fixed blade relative to the cylinder in the ANSYS WORKBENCH software. Using the three-dimensional modeling system, 4 variants of blades with angles of 0, 30, 45, and 60 degrees were designed. The airflow velocity varied from 3 to 12 m/s [19].



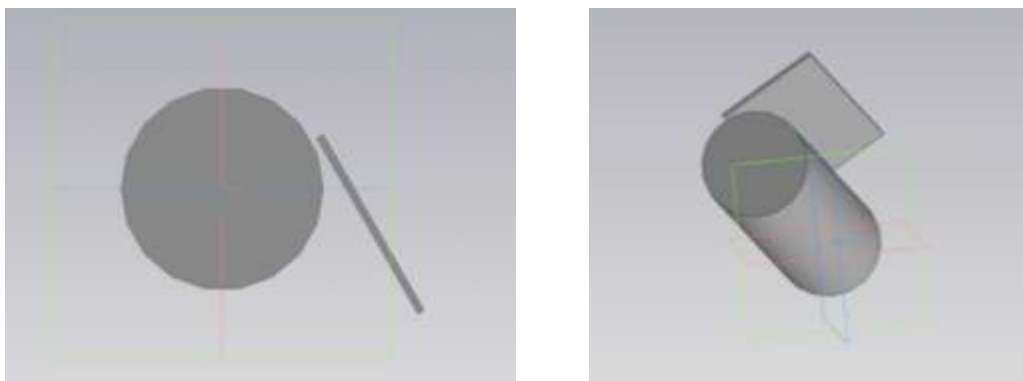
a) 0 degree



b) 30 degree



c) 45 degree



d) 60 degree

Figure 2. Options for the location of the fixed blade relative to the cylinder

**Numerical study**

**Computing area**

The authors used a method for modeling turbulent flows based on solving averaged Navier Stokes equations (RANS).

With the help of the Enclosure program, a cylindrical computational subdomain was created around the combined blade, with a radius of 0.05 m to set the rotation conditions around the y-axis. To set the boundary conditions around the swept space, a subdomain was created that simulates a wind tunnel in the form of a parallelepiped with dimensions of 1m; 1m; 1.5 m; 1;1;2 m minus the cylindrical subdomain [19] (Fig. 3).

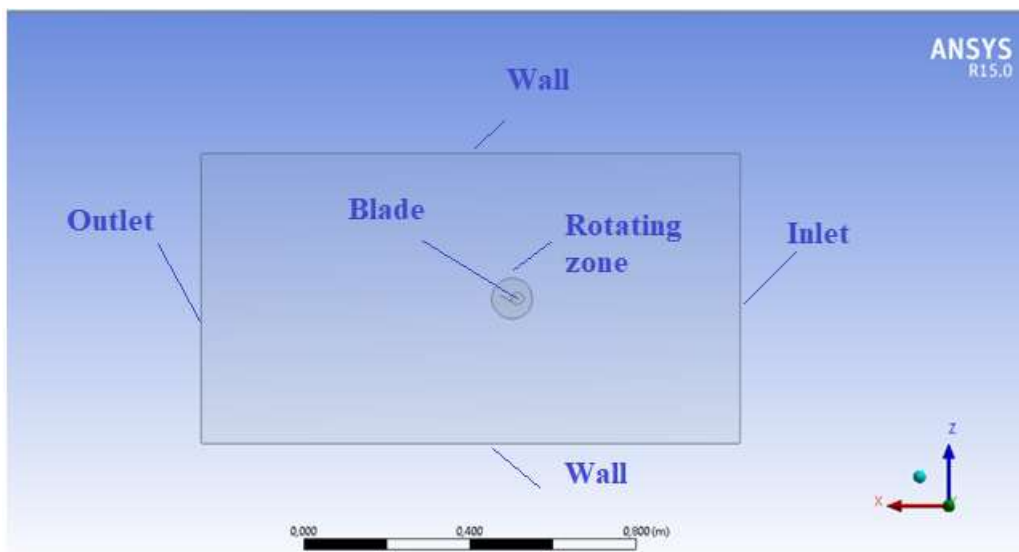


Figure 3. Calculation area

**Boundary conditions**

The following boundary conditions were used in the model [19]:

*Wall (no-slip).* The boundary conditions of the wall (BC) are used to bind the liquid and the solid area. In our case, it will be the surface of the blade and atmospheric air.

*The speed at the entrance.* It is used to determine the set airflow velocity, and it will (3, 5, 7, 10, 12 m/s) together with all the corresponding scalar properties of the flow, as a turbulent model at the entrance to the flow. The total pressure is not fixed but will rise to any value necessary to ensure the necessary velocity distribution.

*Rotation of the blade.* Is a periodic boundary condition, and is equal to 300, 500, and 700 rpm.

**Turbulence model**

The problem was solved in a stationary setting. To solve the problem of computer modeling, three-dimensional Reynolds-averaged Navier-Stokes equations were numerically integrated. To close the

equations of motion, the Realizable k- $\epsilon$  turbulence model, which proved itself well on a wide class of problems, was taken, and a viscous incompressible gas (air) was used as a working medium.

#### **Aerodynamic coefficients**

An indicator of the efficiency of an aerodynamic element is the aerodynamic coefficients. Using formulas (1) and (2), the aerodynamic coefficients are calculated by numerical method [4].

The drag coefficient is calculated by the formula (1):

$$C_x = \frac{2F_x}{\rho u^2 S} \quad (1)$$

The lift coefficient is calculated by the formula (2):

$$C_y = \frac{2F_y}{\rho u^2 S} \quad (2)$$

where,  $F_x$  is the drag force, H;  $F_y$  — lifting force, H;  $\rho$  — air density, kg/m<sup>3</sup>;  $u$  — flow rate, m/s;  $S$  — the area of the midsection, m<sup>2</sup>.

#### *Results and Discussion*

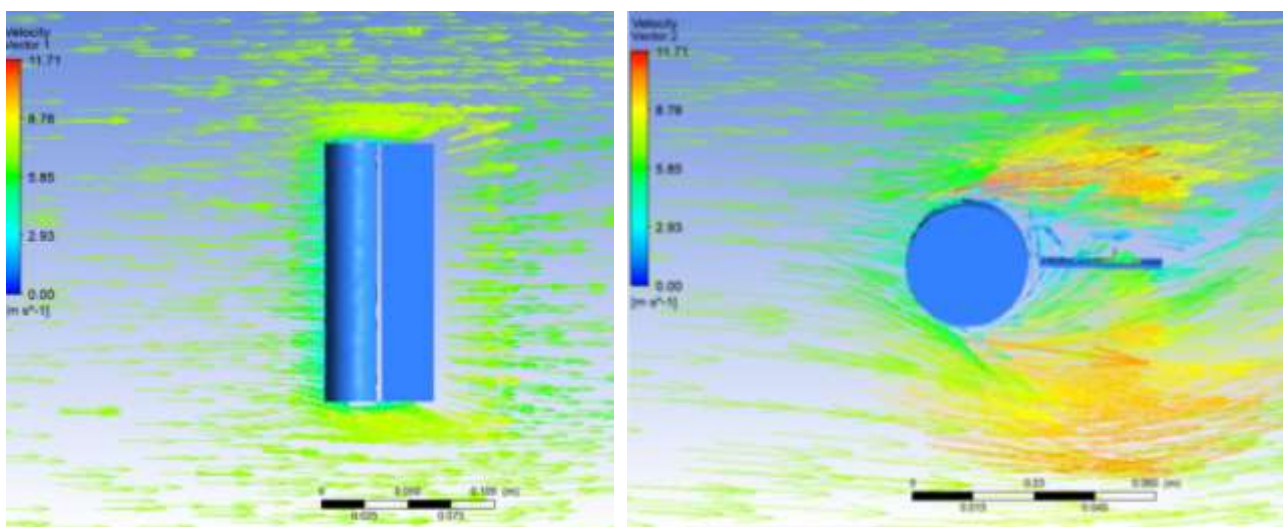
As a result of numerical simulation, the results of the distribution pattern of velocity vectors around the combined blade at  $u=7$  m/s,  $n=500$  rpm are obtained (Fig. 4).

In the upper left corner, there is a color gradation from blue (minimum) to red (maximum), which is a panel of symbols.

From Figure 4 defined, the angle of inclination of the fixed blade has a great influence on the overall picture of the time-averaged velocity vectors. As the angle of inclination of the blade increases, the turbulence between the cylinder and the blade increases. The so-called closed space is created, which, with increasing angle, becomes more closed and gives more resistance when flowing around the airflow. It is determined that when the fixed blade is positioned at an angle of 0 degrees to the cylinder, a maximum flow velocity of about 11.71 m/s is observed, which is an assumption about the most effective location of the fixed blade.

Figure 5 shows the results of the static pressure distribution field ( $p_{st} = p - p_{atm}$ ) around the combined blade at  $u=7$  m/s,  $n=500$  rpm.

From the Figure 5 defined, when the angle of the fixed blade is 0 degrees, the so-called additional repulsion of the entire combined blade occurs, due to the formation of high pressure behind the fixed blade. Thus, an additional lifting force of the most stationary blade is formed.



a) 0 degrees

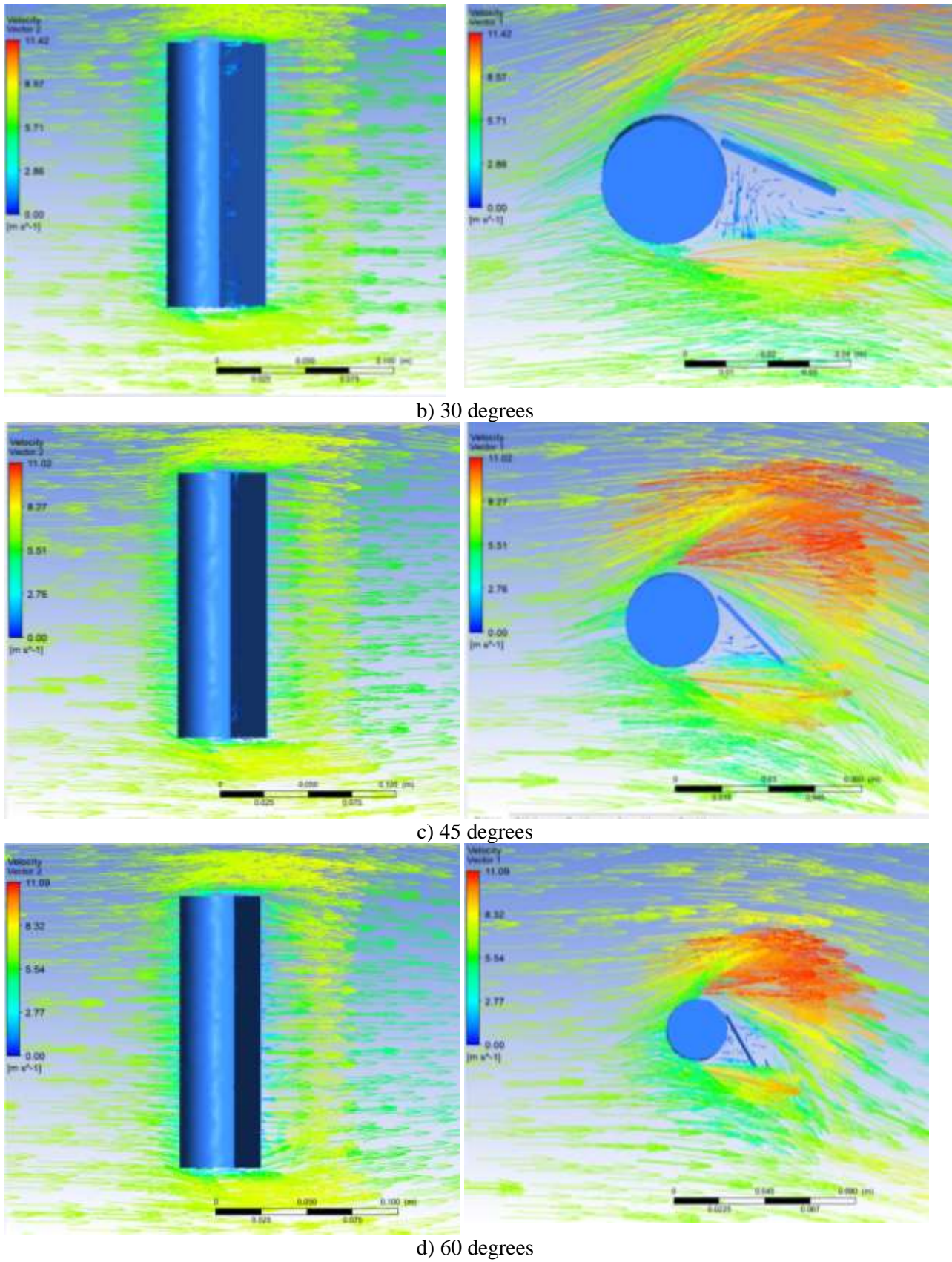
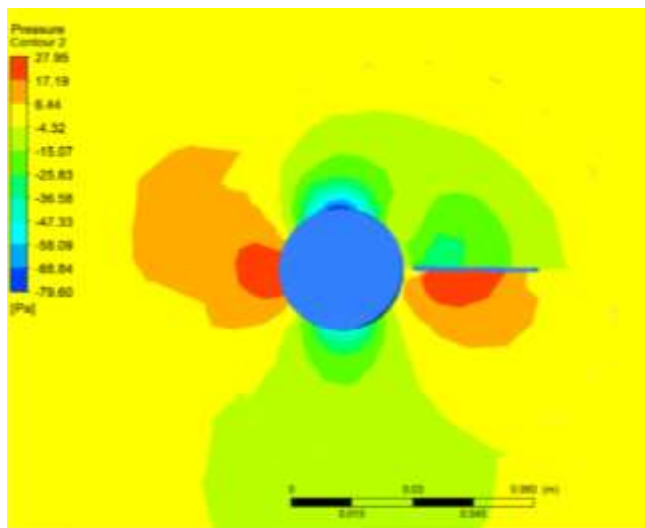
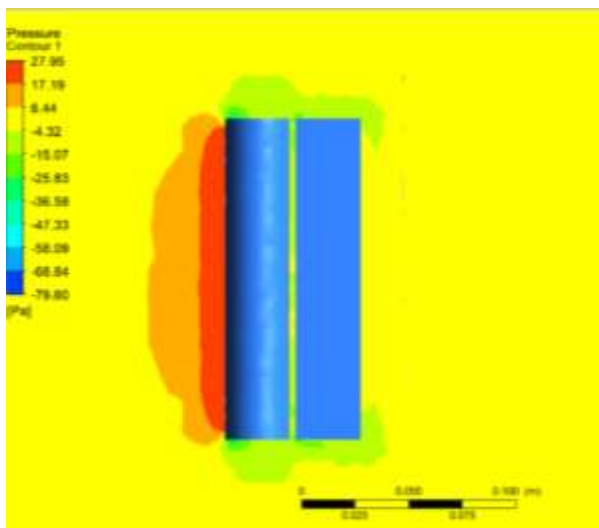
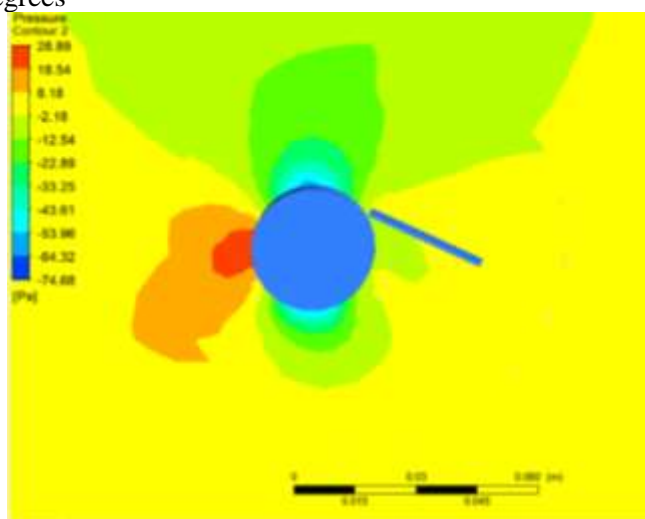
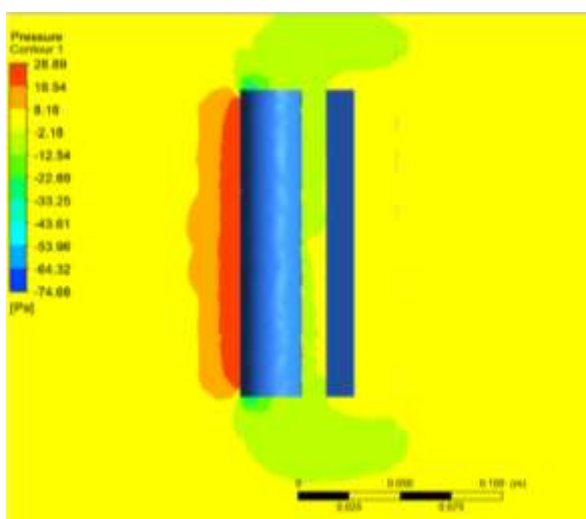


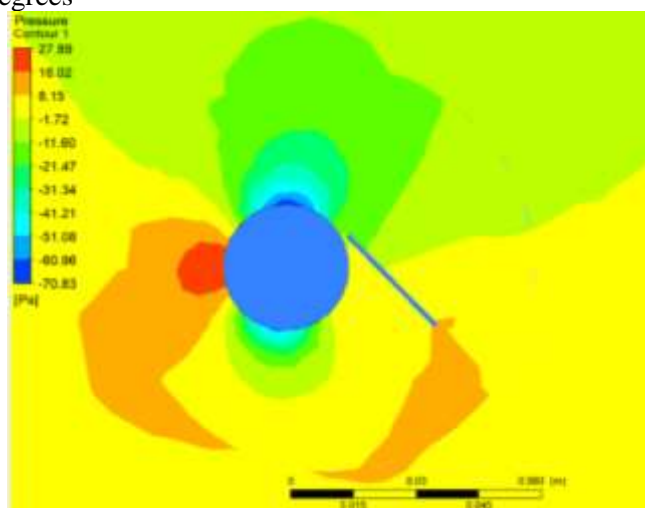
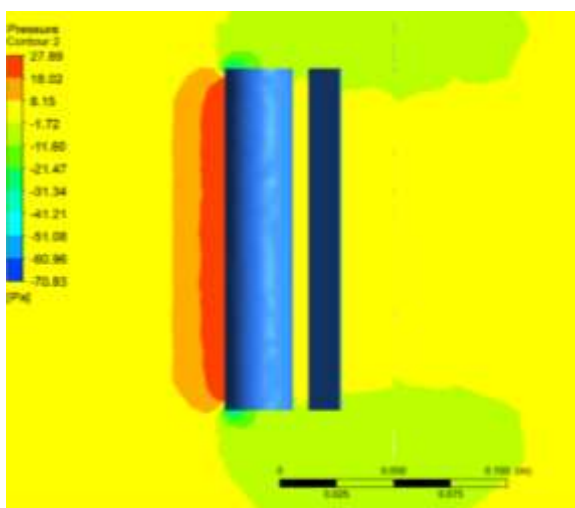
Figure 4. Time-averaged velocity vectors around the combined blade at  $u = 7$  m/s,  $n = 500$  rpm



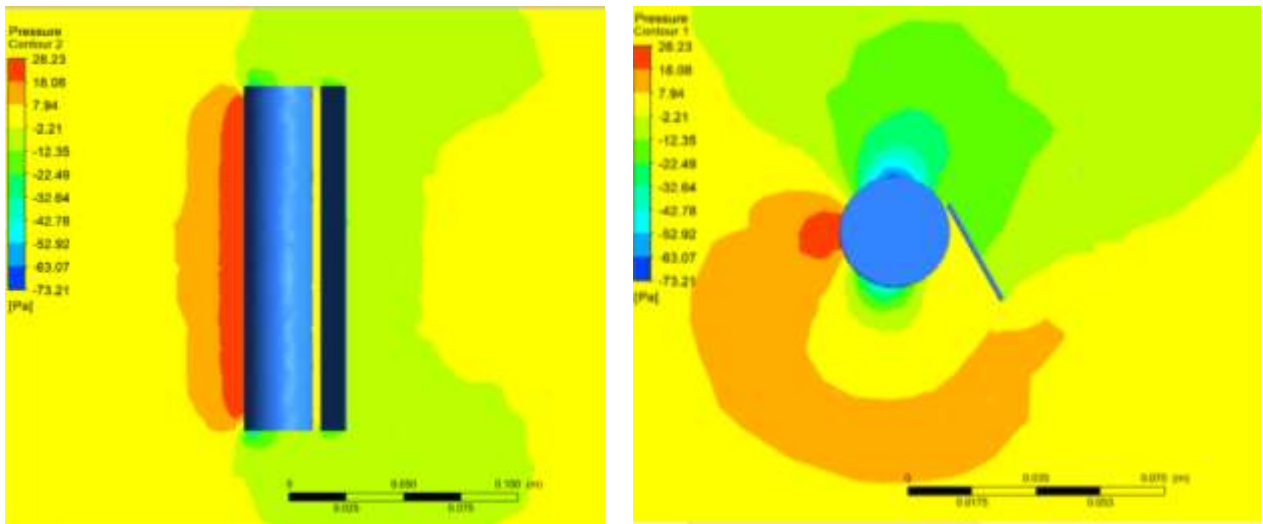
0 degrees



30 degrees



45 degrees



60 degrees

Figure 5. Pressure fields around the combined blade at  $u = 7$  m/s,  $n=500$  rpm

Figures 6 and 7 present the results of the numerical calculation of the lift coefficient and drag force from the Reynolds number for various variants of the fixed blade relative to the cylinder.

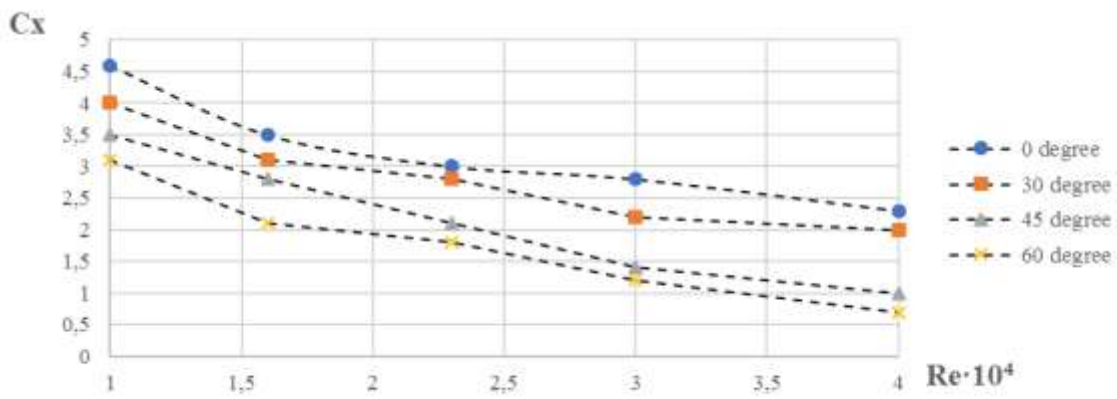


Figure 6. Line graph showing the change in drag coefficient from Reynolds

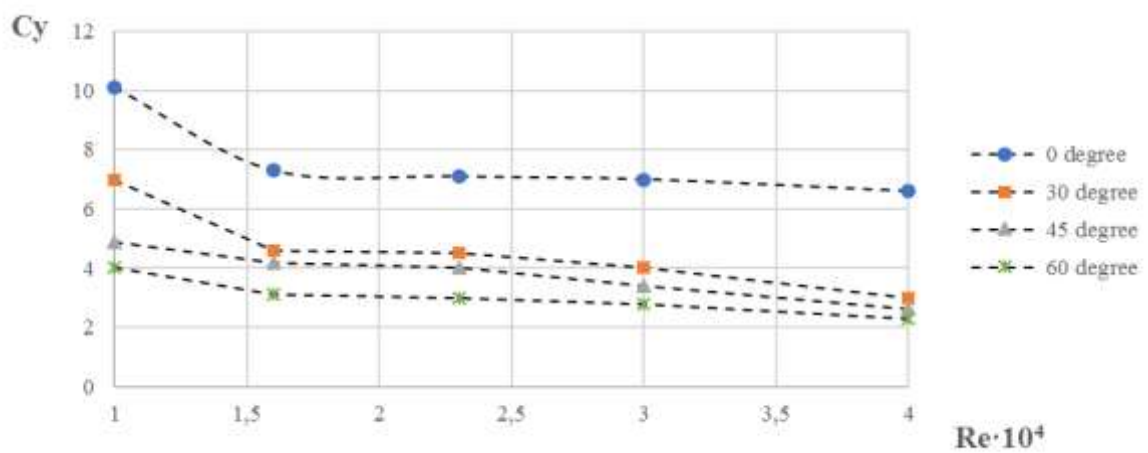


Figure 7. Line graph showing the change in lift coefficient from Reynolds



From the Figures 6 and 7 it is set, when the fixed blade is positioned relative to the cylinder at 0 degrees, the optimal values of the lift and drag coefficients are obtained: 10 and 4.5 with a Reynolds number of  $1 \cdot 10^4$ . Compared with the other three samples at  $30^\circ$ ,  $45^\circ$  and  $60^\circ$ , at  $0^\circ$ , the combined blade produces maximum lift and minimum drag force. Compared with the experimental results of cylinders of different shapes (with a porous surface, with a deflector) [21-22] the obtained numerical data of the lift coefficient is almost 2 times higher, which makes it possible to assert that a combined blade is much more efficient than a single cylindrical blade and a blade from a cylinder with a deflector. Below is the dependence of the number of revolutions of the blade on the wind speed at different angles of attack (Fig. 8).

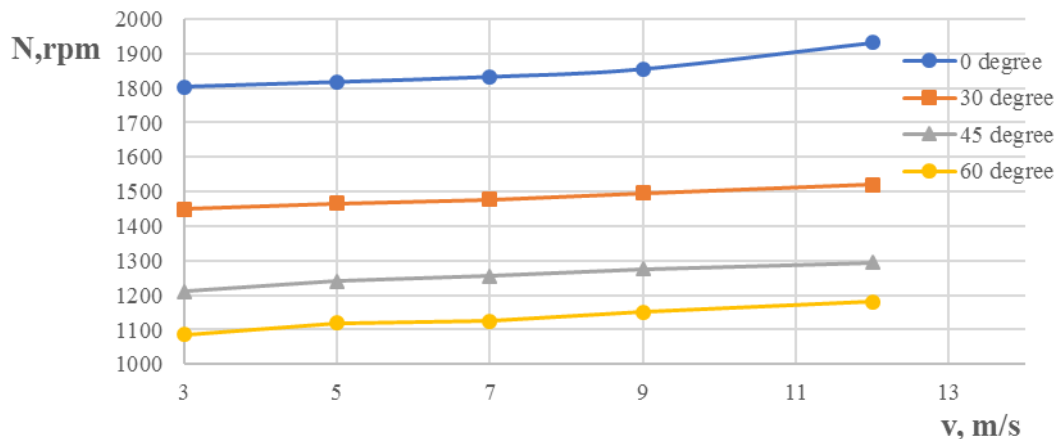


Figure 8. Dependence of rotation speed on wind speed

As can be seen from Figure 8, the number of revolutions of the combined blade is much higher than the number of revolutions of a single cylinder, this is because, during its rotation, the blade carries away adjacent layers of air as a result, the surrounding air receives, in addition to translational motion, rotation around the cylinder, thereby increasing the number of revolutions of rotation.

#### Conclusion

The authors of the article conducted numerical studies using the ANSYS program to determine the optimal location of the fixed blade to the cylinder.

Based on the conducted numerical research:

- the geometry of the combined blade with different angles of the fixed blade:  $0^\circ$ ;  $30^\circ$ ;  $45^\circ$  and  $60^\circ$  have been created. The Realizable  $k-\varepsilon$  model was used as a turbulence model. The flow rate varied from 3–12 m/s;
- three-dimensional pictures of the velocity distribution and the static pressure field around the blade are obtained. It is established that with an increase in the angle of the fixed blade, the turbulence between the cylinder and the blade increases. It is determined that as the angle increases, the pressure in the space between the cylinder and the blade disappears, which is also an additional lifting force;
- from the dependence of the coefficient of lift and drag force on the Reynolds number, it was found that at an angle of  $0^\circ$  degrees, there is a maximum lifting force of 10 and a minimum drag force of 4.5 at  $Re = 1 \cdot 10^4$ .

- It is established that at a wind speed of 12 m/s and an angle of attack of 0 degrees, the number of revolutions of the blade is 1932 rpm.

- It was found that with the angle of the fixed blade  $0^\circ$  degrees, the indicators of the entire combined blade are the most effective.

#### Acknowledgments

The work was carried out with the financial support of the Science Committee of the Ministry of Science and Higher Education of the Republic of Kazakhstan (IRN AP14972704 “Numerical study of a new design of wind turbine blades with a horizontal axis of rotation”).

## References

- 1 Jureczko, M., Pawlak, M., & Męzyk, A. (2005). Optimization of wind turbine blades. *Journal of materials processing technology*, 167(2-3), 463–471.
- 2 Balat, M. (2009). A review of modern wind turbine technology. *Energy Sources, Part A*, 31(17), 1561–1572.
- 3 Saad, M.M.M., & Asmuin, N. (2014). Comparison of horizontal axis wind turbines and vertical axis wind turbines. *IOSR Journal of Engineering (IOSRJEN)*, 4(08), 27–30.
- 4 Tanasheva, N.K., Bakhtybekova, A.R., Shaimerdenova, G.S., Sakipova, S.E., & Shuyushbaeva, N. (2022). Modeling aerodynamic characteristics of a wind energy installation with rotating cylinder blades on the basis of the ansys suite. *Journal of Engineering Physics and Thermophysics*, 95(2), 457–463.
- 5 Sanusi, A., Soeparman, S., Wahyudi, S., & Yuliati, L. (2016). Experimental study of combined blade savonius wind turbine. *International Journal of Renewable Energy Research (IJRER)*, 6(2), 614–619.
- 6 Chauhan, M.K., Dutta, S., More, B.S., & Gandhi, B.K. (2018). Experimental investigation of flow over a square cylinder with an attached splitter plate at intermediate Reynolds number. *Journal of Fluids and Structures*, 76, 319–335.
- 7 Zhu, H., Li, G., & Wang, J. (2020). Flow-induced vibration of a circular cylinder with splitter plates placed upstream and downstream individually and simultaneously. *Applied Ocean Research*, 97, 102084.
- 8 Assi, G.R.S., & Bearman, P.W. (2015). Transverse galloping of circular cylinders fitted with solid and slotted splitter plates. *Journal of Fluids and Structures*, 54, 263–280.
- 9 Zeng, L., Zhao, F., Wang, H., Liu, Y., & Tang, H. (2023). Control of flow-induced vibration of a circular cylinder using a splitter plate. *Physics of Fluids*, 35(8).
- 10 Wu, B., Li, S., Li, K., & Zhang, L. (2020). Numerical and experimental studies on the aerodynamics of a 5: 1 rectangular cylinder at angles of attack. *Journal of Wind Engineering and Industrial Aerodynamics*, 199, 104097.
- 11 Neelapu, T.R., Neelapu, K.A., & Kumar, S.A. (2022). Influence of Wake Splitter Plate on Flow Over a Triangular Cylinder at a Low Reynolds Number: A Numerical Study. In *Biennial International Conference on Future Learning Aspects of Mechanical Engineering* (pp. 517–527). Singapore: Springer Nature Singapore.
- 12 An, B., Bergada, J.M., Mellibovsky, F., Sang, W.M., & Xi, C. (2020). Numerical investigation on the flow around a square cylinder with an upstream splitter plate at low Reynolds numbers. *Meccanica*, 55, 1037–1059.
- 13 Li, S., Li, M., Wu, B., Li, K., & Yang, Y. (2023). Three-dimensional aerodynamic lift on a rectangular cylinder in turbulent flow at an angle of attack. *Journal of Fluids and Structures*, 118, 103859.
- 14 Pfister, J.L., & Marquet, O. (2020). Fluid–structure stability analyses and nonlinear dynamics of flexible splitter plates interacting with a circular cylinder flow. *Journal of Fluid Mechanics*, 896, A24.
- 15 Sun, X., Suh, C.S., Ye, Z.H., & Yu, B. (2020). Dynamics of a circular cylinder with an attached splitter plate in laminar flow: A transition from vortex-induced vibration to galloping. *Physics of Fluids*, 32(2).
- 16 Sharma, K.R. & Dutta, S. (2020). Flow control over a square cylinder using attached rigid and flexible splitter plate at intermediate flow regime. *Physics of Fluids*, 32(1).
- 17 Zhu, H., Chen, Q., Tang, T., Alam, M.M., & Zhou, T. (2023). Flow structures around a circular cylinder with bilateral splitter plates and their dynamic characteristics. *Ocean Engineering*, 269, 113547.
- 18 Tanasheva, N.K., Bakhtybekova, A.R., Shuyushbayeva, N.N., Tussupbekova, A.K., & Tleubergenova, A.Z. (2022). Calculation of the aerodynamic characteristics of a wind-power plant with blades in the form of rotating cylinders. *Technical Physics Letters*, 48(2), 51–54.
- 19 Dyusembaeva, A.N., Tleubergenova, A.Z., Tanasheva, N.K., Nussupbekov, B.R., Bakhtybekova, A.R., & Kyzdarbekova, S.S. (2023). Numerical investigation of the flow around a rotating cylinder with a plate under the subcritical regime of the Reynolds number. *International Journal of Green Energy*, 1–15.
- 20 Oh, G., Park, H., & Choi, J.I. (2022). Drag, lift, and torque coefficients for various geometrical configurations of elliptic cylinder under Stokes to laminar flow regimes. *AIP Advances*, 12(6).
- 21 Tanasheva, N.K., Shuyushbayeva, N.N., & Mussenova, E.K. (2018). Studying the dependence of the aerodynamic characteristics of rotating cylinders on the rake angle of air flow. *Technical Physics Letters*, 44, 787–789.
- 22 Bakhtybekova, A.R., Tanasheva, N.K., Minkov, L.L., Shuyushbayeva, N.N., & Dyusembaeva, A.N. (2022). Aerodynamic features of a rotating cylinder with a deflector. *Journal of Applied Mechanics and Technical Physics*, 63(5), 833–842.

А.Н. Дюсембаева, Н.К. Танашева, А.Ж. Тлеубергенова, А.Р. Бахтыбекова,  
Ж.Б. Кутумова, А.Р. Тусупханова, Н.Т. Абдилова

### Сандық әдісті қолдана отырып жел энергетикалық қондырғысының ротор қалақшасының геометриялық пішінін оңтайлы таңдау

Жел турбиналарының энергия тиімділігін арттыру үшін қалақтар түріндегі күштік элементтерінің пішіні мен өлшемдерін оңтайландыру және жақсарту қажет. Жұмыста алынған энергетикалық және шығу көрсеткіштерін жақсарту және үлкейту, сондай-ақ көтеру күшін арттыру мақсатында айналмалы

цилиндр және қозғалмайтын қалақша түріндегі құрамалы қалақша жасалды және сандық түрде зерттелді. Жұмыстың жаңалығы 3-тен 12 м/с-қа дейінгі ауа ағынының жылдамдығы кезінде барлық біріктірілген қалақтың (цилиндр және қозғалмайтын қалақша) жалпы аэродинамикалық сипаттамаларына көлбеу бекітілген қалақ бұрышының әсерінің сандық нәтижелерінің алынуында. Үш өлшемді сандық модельдеу негізінде қозғалмайтын қалақшаның әртүрлі орналасу бұрыштары бар құрамалы қалақшаның 4 нұсқасы жобаланған. Турбуленттілік моделі ретінде *Realizable k-ε* моделі қолданылды, ол есептердің кең класында өзін дәлелдеді, ал жұмыс ортасы ретінде тұтқыр сығылмайтын газ (ауа) қолданылды. Жылдамдық векторлары мен қысым өрістерінің таралуының үш өлшемді суреттері алынды. Нәтижелерден қозғалмайтын қалақша  $0^\circ$  бұрышта орналасқан кезде құйындылардың ең аз түзілуі байқалатыны айқындалды. Аэродинамикалық коэффициенттердің Рейнольдс санына тәуелділігінің сызықтық графиктері көрсетілген.  $0$  градус бұрыш кезінде құрамалы қалақшаның ең жоғары көтеру күшінің коэффициенті  $10$  және Рейнольдс  $1 \cdot 10^4$  кезінде ең төмен маңдайлық кедергі коэффициенті  $4,5$  болатыны анықталды. Алынған сандық нәтижелер Магнус эффектісі негізінде жұмыс істейтін құрамалы қалақшалары бар жел энергетикалық қондырғыларын әзірлеуде пайдалы болады.

*Кілт сөздер:* жел энергетикалық қондырғы, құрамалы қалақша, цилиндр, Магнус эффектісі, геометриялық пішін, аэродинамикалық күш, үш өлшемді модельдеу, Рейнольдс саны.

А.Н. Дюсембаева, Н.К. Танашева, А.Ж. Тлеубергенова, А.Р. Бахтыбекова,  
Ж.Б. Кутумова, А.Р. Тусупханова, Н.Т. Абдинова

### Оптимальный выбор геометрической формы лопасти ротора ветроэнергетической установки с использованием численного метода

Для повышения энергоэффективности ветряных турбин необходимо оптимизировать и улучшить форму и размеры силовых элементов в виде лопастей. В данной работе с целью улучшения и увеличения получаемых энергетических и выходных показателей, а также роста подъемной силы была создана и численно исследована комбинированная лопасть в виде вращающегося цилиндра и неподвижной лопасти. Новизна работы заключается в получении численных результатов влияния фиксированного угла наклона лопасти на общие аэродинамические характеристики всей комбинированной лопасти (цилиндра и неподвижной лопасти) при скоростях воздушного набегающего потока от 3 до 12 м/с. На основе трехмерного численного моделирования спроектированы 4 варианта комбинированной лопасти с разными углами расположения неподвижной лопасти. В качестве модели турбулентности использовалась *Realizable k-ε* модель, которая хорошо зарекомендовала себя в широком классе задач, и в качестве рабочей среды использовался вязкий несжимаемый газ (воздух). Получены трехмерные картины распределения векторов скорости и полей давления. Из результатов установлено, что при расположении неподвижной лопасти под углом  $0^\circ$  наблюдается наименьшее образование вихрей. Показаны линейные графики зависимости аэродинамических коэффициентов от числа Рейнольдса. Было обнаружено, что при угле  $0$  градусов комбинированная лопасть имеет максимальный коэффициент подъемной силы  $10$  и минимальный коэффициент лобового сопротивления  $4,5$  при Рейнольдсе  $1 \cdot 10^4$ . Полученные численные результаты будут полезны при разработке и создании ветроэнергетических установок с комбинированными лопастями, работающих на основе Магнус.

*Ключевые слова:* ветроэнергетическая установка, комбинированная лопасть, цилиндр, эффект Магнуса, геометрическая форма, аэродинамическая сила, трехмерное моделирование, число Рейнольдса.

#### Information about authors

**Dyusembaeva, Ainura** — PhD, Associate professor, Department of Engineering Thermophysics, Karaganda Buketov University, Karaganda, Kazakhstan; e-mail: [aikabesoba88@mail.ru](mailto:aikabesoba88@mail.ru). ORCID ID: <https://orcid.org/0000-0001-6627-7262>;

**Tanasheva, Nazgul** — PhD, Associate professor, Department of Engineering Thermophysics, Karaganda Buketov University, Karaganda, Kazakhstan; e-mail: [nazgulya\\_tans@mail.ru](mailto:nazgulya_tans@mail.ru), ORCID ID: <https://orcid.org/0000-0003-4273-0960>;

**Tleubergenova, Akmaral** — 3<sup>rd</sup> year doctoral student, Department of Engineering Thermophysics, Karaganda Buketov University, Karaganda, Kazakhstan; e-mail: [akmaral.tzh7@mail.ru](mailto:akmaral.tzh7@mail.ru), ORCID ID: <https://orcid.org/0000-0003-0316-4222>;

**Bakhtybekova, Assem** (corresponding author) — PhD, Department of Engineering Thermophysics, Karaganda Buketov University, Karaganda, Kazakhstan; e-mail: [asem.alibekova@inbox.ru](mailto:asem.alibekova@inbox.ru), ORCID ID: <https://orcid.org/0000-0002-2018-8966>;

**Kutumova, Zhibek** — Master of natural sciences, Senior lecturer, Department of physics and nano-technology, Karaganda Buketov University, Karaganda, Kazakhstan; e-mail: [zhibek\\_kutumova@mail.ru](mailto:zhibek_kutumova@mail.ru);

**Tussuphanova, Aigerim** — Master of natural sciences, Lecturer, Department of Engineering Thermodynamics, Karaganda Buketov University, Karaganda, Kazakhstan; e-mail: [aigera\\_aigerim@mail.ru](mailto:aigera_aigerim@mail.ru);

**Abdirova, Nurgul** — Master of pedagogical sciences, Lecturer, Department of Engineering Thermodynamics, Karaganda Buketov University, Karaganda, Kazakhstan; e-mail: [abdirova\\_nurgul@mail.ru](mailto:abdirova_nurgul@mail.ru).